Transactions, SMiRT-25
Charlotte, NC, USA, August 4-9, 2019
Division VII

IMPACT OF SCALING THE USNRC AND NBK DESIGN BASIS RESPONSE SPECTRA ON EVALUATION OF HIGH FREQUENCY SENSITIVE COMPONENTS

Amitabh Dar[1] and Wael W. El-Dakhakhani[3]

[1] Technical Advisor, Bruce Power, Canada. Doctoral Researcher, McMaster University, Hamilton, ON, L8S 4L7, Canada (dara@mcmaster.ca)
[2] Professor and University Scholar, Department of Civil Engineering and the School of Computational Science & Engineering, McMaster University, Hamilton, ON, L8S 4L7, Canada

ABSTRACT

The design basis earthquake (DBE) response spectrum for Nuclear Power Plants (NPPs) recommended by the United States Nuclear Regulatory Commission (USNRC) Regulatory Guide 1.60 is based on the so-called NBK spectrum, named after its creators: Newmark, Blume and Kapur. The two spectra are identical in the horizontal direction, but the DBE spectrum is more conservative in the vertical direction for frequencies beyond 33 Hz. For the purpose of seismic margin assessment or probabilistic risk assessment, in-structure response spectra are generated for the review level earthquake (RLE) or the uniform hazard response spectrum (UHRS) by scaling the DBE of the NPPs situated on rock sites in accordance with the methodology given in the Seismic Fragility Application Guide (EPRI 1002988). The conservatism in the vertical DBE spectrum over the high frequency range, based on the USNRC Regulatory Guide 1.60, gets further amplified in form of in-structure response spectra, especially for the east coast sites subjected to high frequency content in the RLE or the UHRS. The conservatism in the amplified response to the vertical excitation adversely impacts the seismic risk of high-frequency sensitive components installed close to columns or shear walls. This paper compares the in-structure response spectra generated by scaling of the USNRC and NBK spectra in the vertical direction. It is concluded that the seismic risk is artificially amplified by double counting the inherent conservative of the USNRC response spectrum over high frequencies. For the examples considered, it is observed that the amplification of vertical peak accelerations through the height of a structure is coupled with the reduction in peak frequency, implying that the high frequency sensitive components located at higher elevations may not be at risk. In contrast to EPRI report 3002004396, amplification of high frequency acceleration was found to be much more prominent at lower elevations rather than higher ones. An investigation on coupling of amplification factors with frequency shift through the height of the structure is warranted to be included in EPRI report 3002004396.

INTRODUCTION

The design basis response spectrum for NPPs created by Newmark, Blume and Kapur (Newmark et al., 1973), popularly known as the NBK spectrum, is based on western US earthquakes. It was adopted in the USNRC Regulatory Guide 1.60 Revision 01 (USNRC, 1973) and maintained in its Revision 02 (USNRC, 2014) but with added conservatism in vertical direction over high frequencies. The USNRC spectrum was adopted as the design basis of some NPPs in eastern Canada and the central eastern US, addressed together as East North America (ENA) hereinafter. Later, several earthquakes records, especially Saguenay 1988 earthquake as a classic example, highlighted the difference between the frequency content of the ENA earthquakes (Atkinson & Elgohary, 2007) and their western counterparts. While the USNRC spectrum is rich over low frequencies (2-10 Hz) and deficient over the higher ones, a typical ENA spectrum is quite the

opposite. Figure 1(a) shows comparison of the horizontal USNRC spectrum and a typical ENA UHRS with $1x10^{-4}$ annual probability of exceedence. The difference between the probabilities of the design basis and beyond design basis events can be found in Dar and Hanna (2012) and Dar et al. (2014). Figure 1(b) shows the difference between the horizontal USNRC spectrum and the standard spectrum recommended in the Canadian standard CSA N289.3 (2010). Both spectra are more or less in agreement with each other. The details of the CSA spectrum are beyond the scope of this study and are not discussed further.

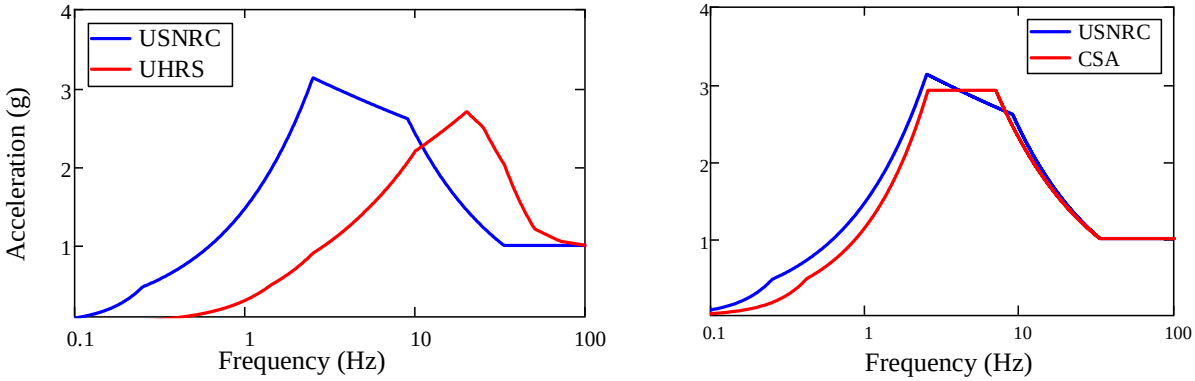

Figure 1: Comparison of 5% damped response spectra normalized to 1g PGA: USNRC Regulatory Guide 1.60 horizontal response spectrum with (a) ENA UHRS, and, (b) CSA spectrum.

Seismic margin assessment (SMA) or seismic probabilistic risk assessment (SPRA) of an NPP requires its evaluation for a site-specific RLE or UHRS respectively. According to NP-6041 (EPRI, 1991), the legacy floor response spectra (FRS) or in-structure-response-spectra of NPPs designed for a DBE can be scaled to obtain the FRS for the RLE (or the UHRS). The EPRI fragility guide 1002988 (EPRI, 2002) and its newer version 3002012994 (EPRI, 2018) outline procedures to obtain the FRS for the UHRS by scaling of the legacy FRS. These guides allow simplified scaling if the two spectral shapes, the DBE and the UHRS, are similar, but recommend detailed scaling if they are not. Since the NBK and the USNRC spectra are practically the same in the horizontal direction, their scaling leads to the same results. However, since the structures are rigid in the vertical direction, they tend to amplify vertical high-frequency spectral accelerations. Such amplification enhances the seismic risk of high-frequency sensitive components especially in regions close to columns and shear walls. The conservatism in the USNRC vertical spectrum over the NBK spectrum is likely to result in lower fragilities of these components. CSA N289.3 (2010) recommends evaluation of impact due to high-frequency content of the site-specific seismic hazard. In order to mitigate the extent of condition for components near rigid supports in an ENA NPP, it is imperative to compare the impact of inherent conservatism in the USNRC spectrum over high frequencies with that of the NBK spectrum in the vertical direction. This paper investigates the difference between the vertical scaling of the USNRC and NBK spectra and its influence on seismic risk. It also suggests improvement in prevailing practices of scaling and vertical seismic amplification reported in the literature.

DEFINITION OF RIGID FREQUENCY

Before delving into further analysis, it is imperative to understand the concept of *rigidity* with respect to a response spectrum. A fixed-base rigid single degree of freedom (SDOF) oscillator replicates its base excitation without any amplification or attenuation. The *rigid frequency* is defined as the lowest frequency beyond which there is no amplification or attenuation of the base excitation. Thus, the lowest frequency in a response spectrum corresponding to its zero period acceleration (ZPA) would be the *rigid frequency*. In Figure 1(a), for the USNRC spectrum, the rigid frequency is 33Hz, whereas, for the UHRS, it is close to100 Hz.

USNRC AND NBK SPECTRA

Figure 2(a) shows the USNRC horizontal response spectrum anchored at acceleration 1g with control frequencies: 0.25, 2.5, 9 and 33Hz, depicted as D, C, B and A respectively. The spectrum is constituted by a set of straight lines joining the control points on a log-log plot. The bottom-most blue line shows the ground motion parameters: peak ground acceleration (PGA) of 1g to the right of point C known as the acceleration sensitive region and peak ground displacement (PGD) of 36 inches to the left of point D, known as the displacement sensitive region. The velocity-sensitive region lies between points D and C. The spectral shapes above ground motion depict damping dependent amplified response, starting from the top, at 0.5%, 2%. 5% and 10% damping. The amplified response is obtained by utilizing amplification factors given in the USNRC Regulatory Guide 1.60. A site-specific DBE spectrum can be obtained by scaling the USRNC spectrum to the site-specific PGA.

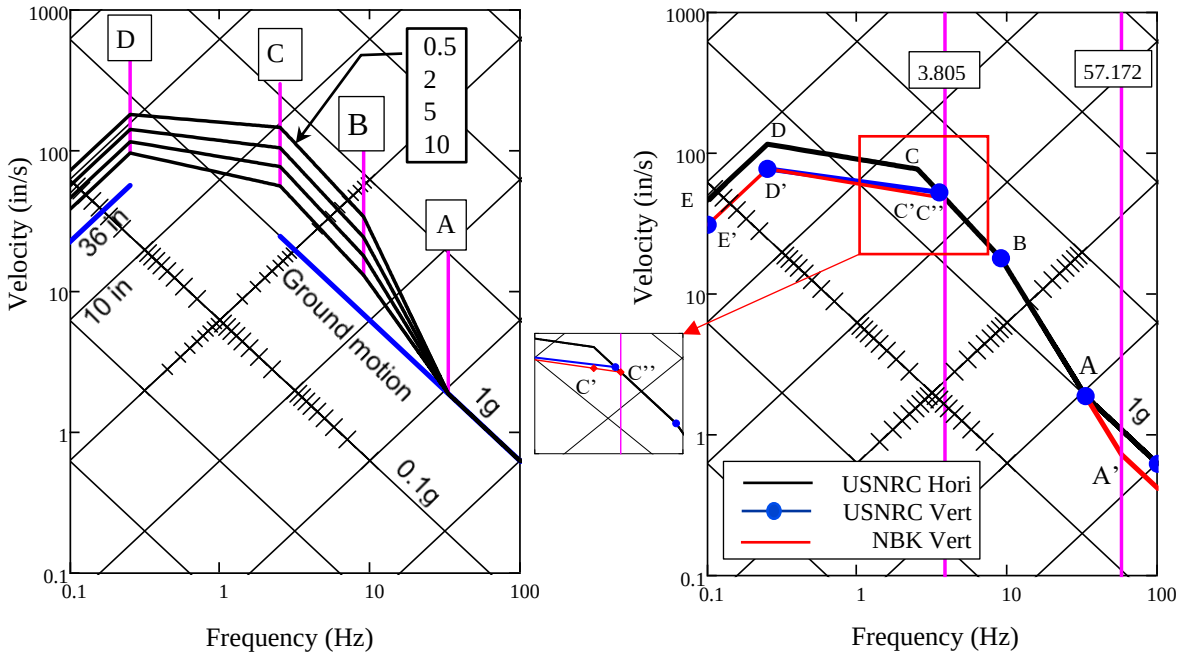

Figure 2: Response spectra anchored at 1g: (a) USNRC horizontal with corner frequencies at A,B,C,D = 33Hz, 9 Hz, 2.5Hz and 0.25Hz respectively at 0.5%, 2%, 5% and 10% damping: (b) USNRC horizontal and vertical with NBK vertical spectra at 5% damping.

Figure 2(b) shows a comparison of the USNRC horizontal (black line) and vertical (blue line and dots) spectra with the NBK vertical spectrum (red line). As illustrated by red lines, for obtaining the vertical NBK response spectrum, Newmark et al. (1973) recommended reduction of the horizontal spectrum by 2/3rd in the displacement (line E'D') and velocity (line D'C') sensitive regions, no reduction in acceleration sensitive region up to 33Hz and again by 2/3rd in the zero period acceleration (ZPA) beyond point A' depicted in red. As illustrated in the inset by red diamond markers, the intersection point C'', at 3.805Hz, is obtained by extending the line D'C' up to the horizontal spectrum. The intersection point, A', at 57.172Hz is obtained by extending the descending branch of the horizontal spectrum (black line between A and B) up to the NBK ZPA (red line) which is 2/3rd of the horizontal ZPA. As evident from Figure 1(b), the lines D'C'C" and DC are parallel and the frequency corresponding to the intersection point C" depends on damping. Thus, the frequencies corresponding to points C" and A' vary with damping. The *rigid frequency* for vertical NBK spectrum at 5% damping in Figure 2(b) is 57.172Hz.

The USNRC Regulatory Guide 1.60 simplified the above procedure by considering 2/3rd reduction in the displacement sensitive region and joining point D' with the horizontal spectral acceleration at 3.5Hz with no further reduction in acceleration. This point (spectral acceleration at 3.5Hz) is depicted as a blue dot in Figure 2(b) and the inset. The blue line close to line D'C'C" is not parallel to DC. Beyond 3.5Hz, vertical response spectrum is exactly the same as horizontal resulting in conservatism over high frequency range beyond 33Hz in comparison to the NBK spectrum.

EQUATIONS FOR THE USNRC AND NBK SPECTRA

Horizontal Spectra

According to Newmark at al. (1973), the generic response spectrum (Figure 2(a)) can be scaled to the site-specific PGA. The scaling factors at points B, C and D are (Newmark at al. 1973):

$$S_A^{\mathrm{B}} = 4.25 - 1.02\ln(\beta),$$

$$S_A^{\mathrm{C}} = 5.1 - 1.224\ln(\beta),$$

$$S_A^{\mathrm{D}} = 0.23\big(2.85 - 0.5\ln(\beta)\big)$$

where, S_A^{B}, S_A^{C}, and S_A^{D} are scaling factors and β is the damping ratio expressed as percentage number (e.g. 5 for 5% damping). The displacement factor at point D, given in Newmark et al. (1973) has been converted to the acceleration scaling factor, S_A^{D} in the above equation. The control points (A, B, C and D) of the horizontal spectrum can be obtained by multiplying the site-specific PGA by the above factors.

In order to mathematically obtain every point of the response spectrum in between the control points, the following equation from Dar (2014) can be used:

$$S_A = I.\left(\frac{f}{f_r}\right)^s$$

Where, f is the frequency variable, f_r is the larger of the two frequencies defining the control point interval ($r = \mathrm{D}$ for the first interval, C for the second and so on) and S_A is the spectral acceleration in g. Table 1 provides values of I and s for the given frequency ranges with the frequencies: f_{E}=0.1Hz, f_{D}=0.25Hz, f_{C}=2.5Hz, f_{B}=9Hz and f_{A}=33Hz. The spectral acceleration is equal to the PGA for frequencies beyond 33 Hz. An equation written in Mathcad 15.0 (PTC, 2012) on the basis of Table 1 is given in Figure 3(a) with its corresponding functions defined in Figure 3(b) representing spectral accelerations S_A^B, S_A^{C} and S_A^{D}. In these equations, all inputs are dimensionless. For example, to obtain the response acceleration at 2Hz for 0.5g PGA at 5% damping, $\beta = 5$, PGA = 0.5 and f=2.

Table 1: Intercepts and slopes for various frequency intervals (Dar 2014)

	$f_{\mathrm{E}} \le f < f_{\mathrm{D}}$	$f_{\mathrm{D}} \le f < f_{\mathrm{C}}$	$f_{\mathrm{C}} \le f < f_{\mathrm{B}}$	$f_{\mathrm{B}} \le f < f_{\mathrm{A}}$
I	S_A^{D}	S_A^{C}	S_A^B	S_A^{A}=1
s	2	$\log\left(\frac{S_A^{\mathrm{C}}}{S_A^{\mathrm{D}}}\right)$	$1.798\log\left(\frac{S_A^B}{S_A^{\mathrm{C}}}\right)$	$1.772\log\left(\frac{1}{S_A^B}\right)$

Vertical Spectra

Figure 3(c) provides equation for the USNRC vertical spectrum and Figure 3(d) provides the same for the NBK vertical spectrum. Figure 3(e) and (f) provide equations to obtain frequencies at points C'' and A'

(Figure 2(b)) respectively. It is to be noted that in the USNRC spectrum, at 3.5 Hz, the vertical amplification factor is equal to the horizontal. This factor is denoted as BC(β) in Figure 3(b).

$$SA(\beta,PGA,f) := PGA\cdot \begin{cases} 1 & \text{if } f > f_A \\ \left(\frac{f}{f_A}\right)^{1.772\log\left(\frac{1}{B1(\beta)}\right)} & \text{if } f > f_B \\ \left[B1(\beta)\cdot\left(\frac{f}{f_B}\right)^{\left(1.798\cdot\log\left(\frac{B1(\beta)}{C1(\beta)}\right)\right)}\right] & \text{if } f > f_C \\ \left[C1(\beta)\cdot\left(\frac{f}{f_C}\right)^{\left(\log\left(\frac{C1(\beta)}{D1(\beta)}\right)\right)}\right] & \text{if } f > f_D \\ \left[D1(\beta)\left(\frac{f}{f_D}\right)^2\right] & \text{otherwise} \end{cases}$$

(a)

$$A1(\beta) := 1$$

$$B1(\beta) := (4.25 - 1.02\cdot\ln(\beta))$$

$$C1(\beta) := (5.1 - 1.224\ln(\beta))$$

$$D1(\beta) := 0.2301\cdot(2.85 - 0.5\cdot\ln(\beta))$$

$$BC(\beta) := B1(\beta)\cdot\left(\frac{3.5}{9}\right)^{\left(1.798\cdot\log\left(\frac{B1(\beta)}{C1(\beta)}\right)\right)}$$

or

$$BC(\beta) := -1.167\cdot\ln(\beta) + 4.862$$

BC(β) is used in vertical spectrum

(b)

$$SAVU(\beta,PGA,f) := PGA\cdot \begin{cases} 1 & \text{if } f > f_A \\ \left(\frac{f}{f_A}\right)^{1.772\log\left(\frac{1}{B1(\beta)}\right)} & \text{if } f > f_B \\ \left[B1(\beta)\cdot\left(\frac{f}{f_B}\right)^{\left(1.798\cdot\log\left(\frac{B1(\beta)}{C1(\beta)}\right)\right)}\right] & \text{if } f > 3.5 \\ \left[BC(\beta)\cdot\left(\frac{f}{3.5}\right)^{0.873\cdot\log\left[\frac{BC(\beta)}{\left(\frac{2}{3}D1(\beta)\right)}\right]}\right] & \text{if } f > f_D \\ \frac{2}{3}\left[D1(\beta)\left(\frac{f}{f_D}\right)^2\right] & \text{otherwise} \end{cases}$$

(c)

$$SAV(\beta,PGA,f) := PGA\cdot \begin{cases} \frac{2}{3} & \text{if } f > f5v(\beta) \\ \left(\frac{f}{f_A}\right)^{1.772\log\left(\frac{1}{B1(\beta)}\right)} & \text{if } f > f_B \\ \left[B1(\beta)\cdot\left(\frac{f}{f_B}\right)^{\left(1.798\cdot\log\left(\frac{B1(\beta)}{C1(\beta)}\right)\right)}\right] & \text{if } f > f3v(\beta) \\ \frac{2}{3}\left[C1(\beta)\cdot\left(\frac{f}{f_C}\right)^{\left(\log\left(\frac{C1(\beta)}{D1(\beta)}\right)\right)}\right] & \text{if } f > f_D \\ \frac{2}{3}\left[D1(\beta)\left(\frac{f}{f_D}\right)^2\right] & \text{otherwise} \end{cases}$$

(d)

$$f3v(\beta) := 10^{\left[\frac{\log\left[\frac{3}{2}\cdot\frac{B1(\beta)}{C1(\beta)}\cdot\left[\left(\frac{1}{f_B}\right)^{\left(1.798\cdot\log\left(\frac{B1(\beta)}{C1(\beta)}\right)\right)}\cdot(f_C)^{\left(\log\left(\frac{C1(\beta)}{D1(\beta)}\right)\right)}\right]\right]}{\left(\log\left(\frac{C1(\beta)}{D1(\beta)}\right) - 1.798\cdot\log\left(\frac{B1(\beta)}{C1(\beta)}\right)\right)}\right]}$$

(e)

$$f5v(\beta) := f5\cdot 10^{\left[\frac{\log\left(\frac{2}{3}\right)}{(-1.772\cdot\log(B1(\beta)))}\right]}$$

(f)

Figure 3: Response spectra equations: (a) and (b), for horizontal USNRC and NBK spectra with corresponding functions, (c) vertical USNRC spectrum, (d) vertical NBK spectrum, (e) and (f) frequency equations applicable to (d).

Spectra Tables

Tables for the horizontal and vertical USNRC spectra, scaled to the PGA = 0.05g, pertaining to various damping ratios are given in Appendix.

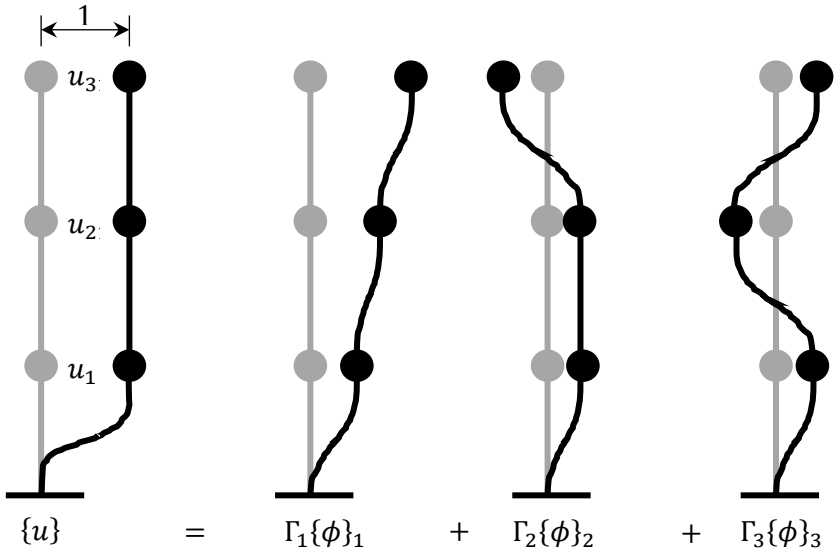

Figure 4: Explanation of participations factors with respect to mode shapes in a 3 DOF system

BRIEF REVIEW OF STRUCTURAL DYNAMICS

The equation of motion of a fixed base single degree of freedom oscillator is given as

$$\ddot{u} + 2\zeta\omega\dot{u} + \omega^2 x = -\ddot{u}_g \tag{1}$$

Where, u is the response of the SDOF oscillator having natural angular frequency, ω, at the damping ratio, ζ, subject to the ground acceleration, $\ddot{u}_g$. In case of multi-degree-of-freedom (MDOF) oscillator shown in Figure 4, the response at node i can be obtained by the equation:

$$u_j = \sum_{j=1}^{m} q_j \phi_{ij} \tag{2}$$

Where, m represents the number of mode shapes, ϕ_{ij} is the mode shape ordinate at node i in mode j. $[\phi]$ is the modal (or mode shape) matrix with n rows (n = number of nodes) and m columns with ϕ_{ij} as its elements. In the modal matrix, the first column $\{\phi\}_1$ represents the first mode, $\{\phi\}_2$ the second and so on. q_j is a time dependent scalar multiplier that can be obtained from the following equation

$$\ddot{q}_j + 2\zeta\omega_j\dot{q}_j + \omega_j^2 q_j = -\Gamma_j\ddot{u}_g \tag{3}$$

Where, Γ_j, the modal participation factor for mode j, is defined in Figure 4. ω_j is modal frequency. The sum $\sum_{j=1}^{m} \Gamma_j\{\phi\}_j = \{1\}$, where, $\{1\}$ is a vector with all elements as 1. This means that the sum of mode shapes multiplied by their respective Γ's leads to unit displacements at each node. Utilizing this definition, Equation (2) turns into

$$\sum_{j=1}^{m} \Gamma_j \phi_{ij} = 1 \text{ for node } i \tag{4}$$

$$\text{or, } \{1\} = [\phi]\{\Gamma\} \tag{5}$$

Where $\{\Gamma\}$ is a vector. This leads to

$$\{\Gamma\} = [\phi]^{-1}\{1\} \tag{6}$$

Generalized mass of mode p is defined as

$$M_{Gp} = \{\phi\}_p^T [M] \{\phi\}_p \tag{7}$$

Equation (6) is useful in computing participation factors directly from the mode shape matrix. Comparing Equations (1) and (3) leads to the fact that Γ_j represents the participation of mode j in capturing Γ_j times the ground motion. Mass normalized modes can be obtained by dividing a mode shape by the square root its generalized mass. From Equation (4), it is seen that a mass normalized participation factor of mode p will be $\Gamma_{Np} = \Gamma_p \sqrt{M_{Gp}}$. In this case the effective mass or the base shear equivalent mass of mode $p = \Gamma_{Np}^2$.

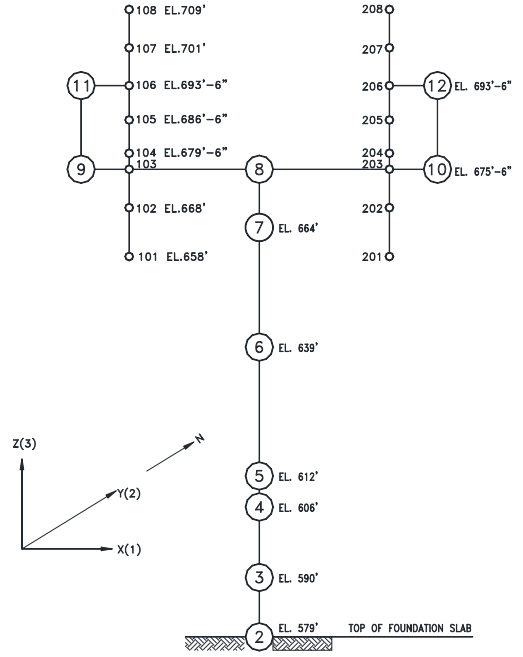

Figure 5: Bruce reactor building example in EPRI guides 1002988 and 3002012994.

BENCHMARK STUDY AT BRUCE SITE AND APPLICABLE SEISMIC EVENTS

The benchmark study example in fragility guides 1002988 (EPRI, 2002) and 3002012994 (EPRI, 2018) is of a reactor building at Bruce site shown in Figure 5. According to the guides, simplified scaling of the legacy FRS is not recommended where the spectral shapes of the UHRS and the legacy DBE are dissimilar. However, the EPRI guides compared the horizontal and vertical FRS for the UHRS obtained by simplified and detailed scaling (addressed as rigorous scaling therein) of the legacy FRS and concluded that the both the methods lead to the same conclusion in horizontal and vertical directions for Bruce site. In order to incorporate high amplification, the EPRI guide chose node 11, i.e., at the highest elevation in the model. The higher elevation nodes are generally not impacted by the higher modes effect which are likely to lead

to high frequency amplification at lower elevation nodes. In this study a lower level node (#4) is chosen to investigate the impact of higher modes on amplification of high frequency excitation. Figure 6 (a) shows 5% damped vertical response spectra at Bruce site: RLE, DBE based on the USNRC spectrum and NBK anchored at 0.1g, 0.05g and 0.033g PGAs respectively. Figure 6(b) shows the 4% damped legacy FRS for the DBE based on the USNRC spectrum in three directions. It is evident that in the horizontal direction, clear peaks are visible and the impact of higher modes is not prominent. Figure 6 (c) shows the 4% damped vertical legacy FRS at node 4 along with 5% damped vertical RLE, USNRC and NBK spectra. If scaled down by the damping ratio ($\sqrt{4/5}$), the legacy FRS practically matches with the USNRC spectrum indicating the influence of higher modes since a high frequency oscillator replicates the base excitation. An artificial time history for the vertical RLE was generated for this study. Figure 6(d) shows the agreement between the response spectra obtained from the artificial time history with that of the vertical RLE.

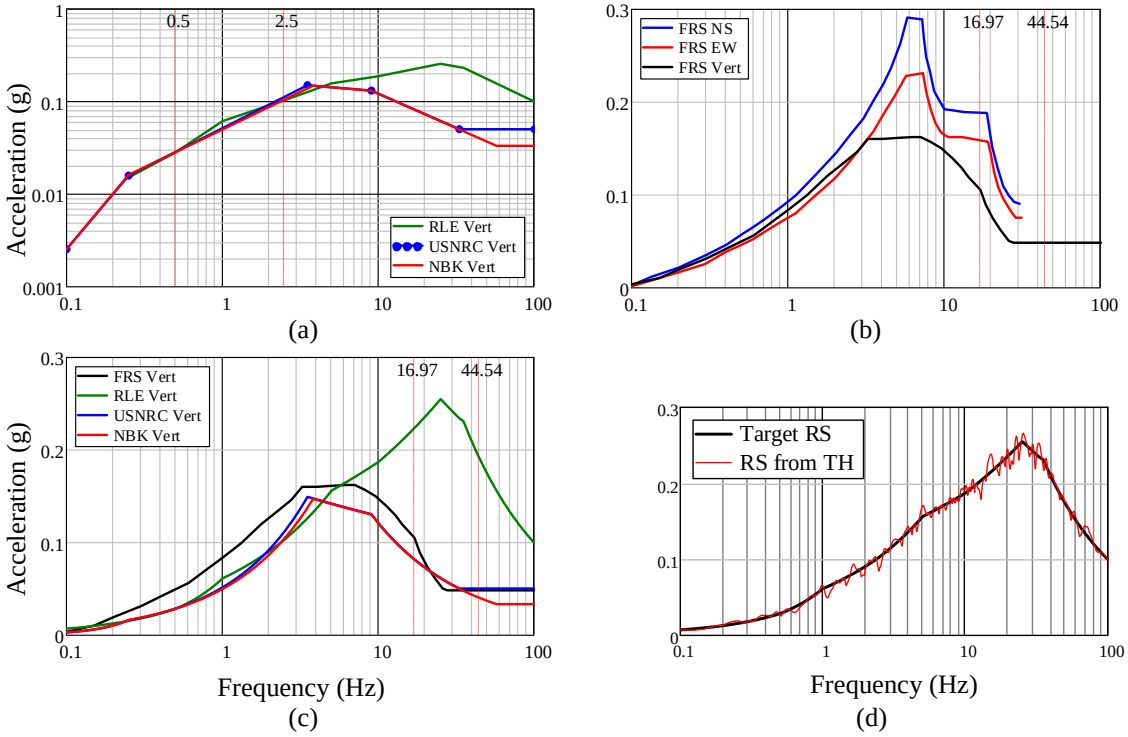

Figure 6: Comparison of response spectra: (a) 5% damped vertical RLE, USNRC and NBK anchored at 0.1g, 0.05g and 0.033g respectively, (b) 4% damped legacy FRS at node 4 in Figure 4 in three directions, (c) 4% damped vertical FRS at node 4 with 5% damped RLE, USNRC and NBK, (d) agreement between the spectrum generated by the time history and the target spectrum of the vertical RLE.

HIGER MODES IMPACT AT LOWER ELEVATION NODES FOR VERTICAL EXCITATION

In order to investigate the impact of higher modes at lower elevation nodes for vertical excitation, a steel column was modeled for six floors with 900 sft tributary area in a steel building and subjected to the artificially time history for the vertical RLE response spectrum (Figure 6 (d)). Figure 7 shows the details of the lumped mass model and vertical mode shapes along with the FRS at various elevations. The vertical grey lines depict modal frequencies: 4.05, 9.4, 14.37, 16.19, 21.76 and 27.98 Hz. It is seen that the FRS at the lowest elevation is highly influenced by the higher modes whereas the FRS at the highest elevation is influenced by lower modes. Amplification is most prominent in the top two (up to 16.10 Hz) and the bottom most nodes (27.98Hz). This behaviour shows that at higher elevations, the high frequency content is filtered out. This is in contradiction with Figure 4-4 of EPRI report 3002004396 (EPRI, 2015) where high frequency amplification is shown to increase with height. In Figure 7, it is interesting to note that the bottom portions

of several FRS closely follow the base excitation (vertical RLE) spectrum. This particular example is included only to demonstrate the higher modes effect at lower nodes and is not discussed further.

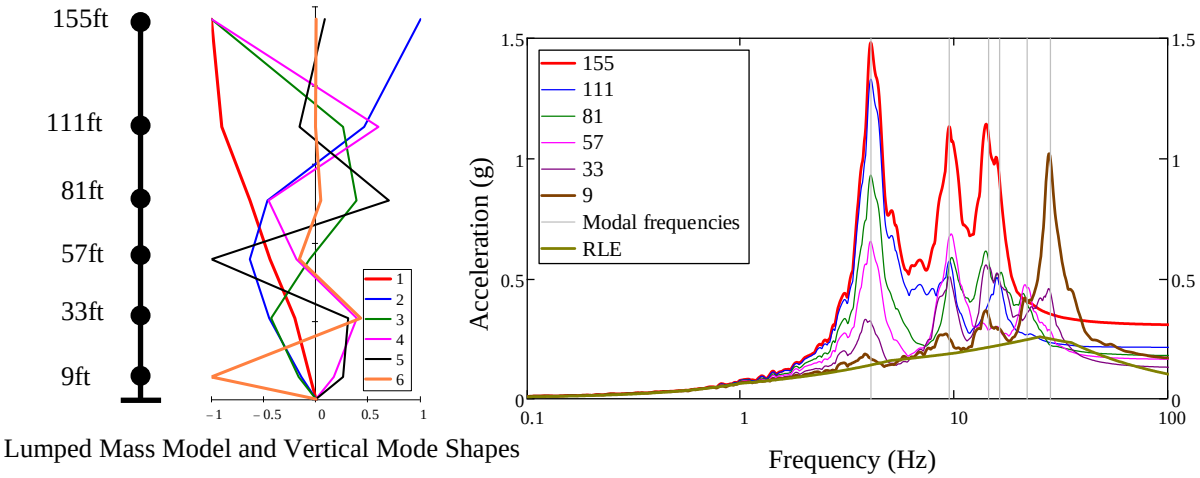

Figure 7: Lumped mass model, vertical mode shapes and FRS at various floors of a steel building

RANDOM VIBRATION THEORY

The fragility guide 3002012994 (EPRI, 2018) recommends utilizing amplification factors from random vibration theory (Crandall & Mark, 1963) for obtaining the FRS at a node by detailed scaling of a given excitation response spectrum. Crandall and Mark (1963) provided white noise solution of two cascaded SDOF oscillators shown in Figure 8 with no feedback from the second to the first. The dynamic properties of the two oscillators in Figure 8 are demarcated with subscripts 1 and 2 for the left and the right oscillator respectively. The left oscillator receives the excitation and its response is transmitted as input to the right oscillator.

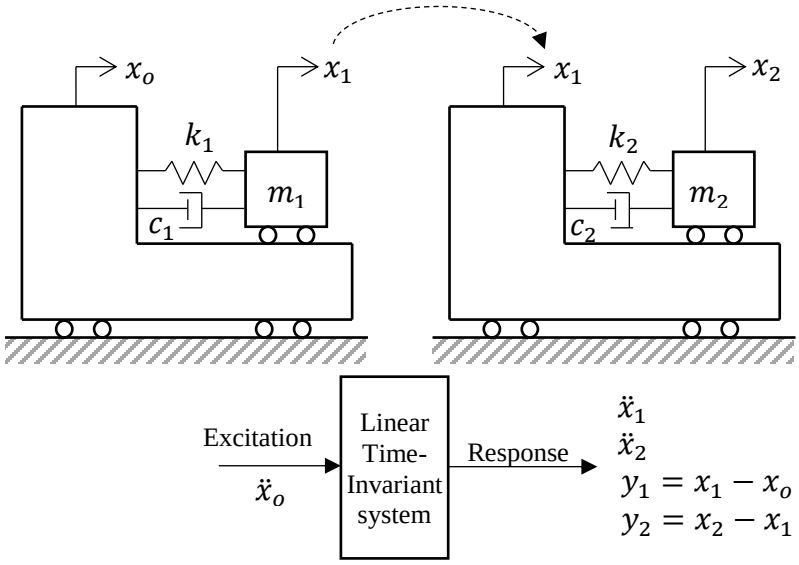

Figure 8: Two cascaded SDOF oscillators (Crandall & Mark, 1963)

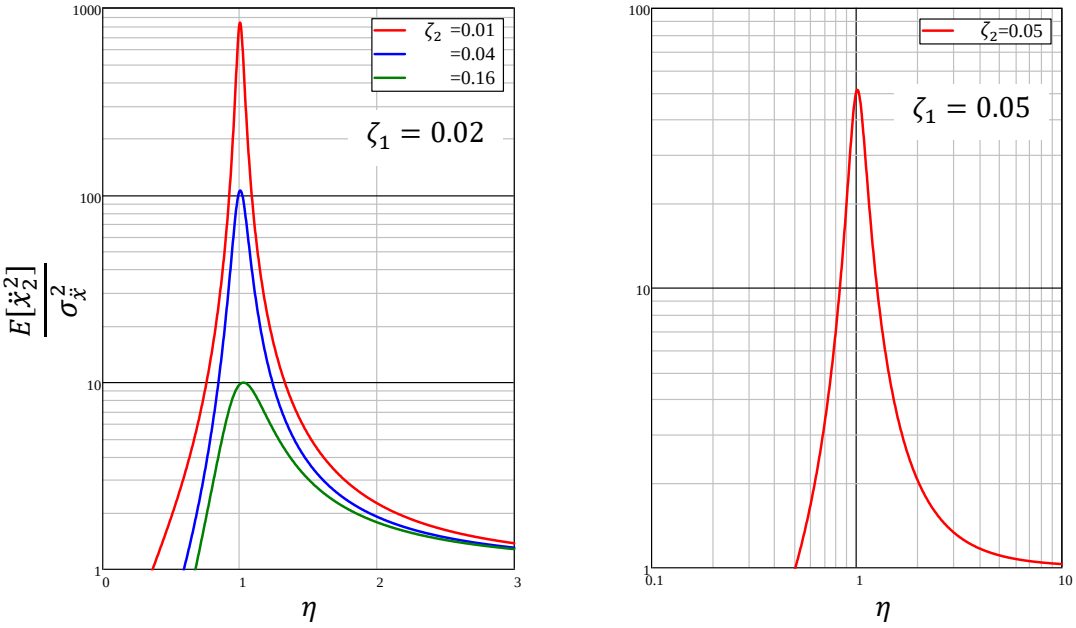

Figure 9: Variation of $E[\ddot{x}_2^2]/\sigma_{\ddot{x}}^2$ with respect to η: The plot on left for $\zeta_1 = 0.02$ matches with Fig. B-1 and the plot on right for $\zeta_1 = 0.05$ matches with Fig. 2.13 (for $\mu = 0$) in Crandall and Mark (1963)

The ratio of angular frequencies of the two oscillator is defined as $\eta = \omega_2 / \omega_1$, their mass ratio as $\mu = m_2 / m_1$ and their damping ratios as ζ_1 and ζ_2 respectively. The mean square response $\left(E\left[\ddot{x}_2^2\right]/\sigma_{\ddot{x}}^2\right)$ charts plotted against η in Crandall and Mark (1963) pertain to various values of μ. For the purpose of developing secondary (amplified by the second oscillator) response spectrum, the charts for $\mu = 0$ are utilized. The ratio, $E[\ddot{x}_2^2]/E[\ddot{x}_1^2]$, represents amplification, by the second oscillator, of its input from the first oscillator. For $\mu = 0$, according to Equations (2.56) and (2.59) in Crandall and Mark (1963), $E[\ddot{x}_1^2] = \sigma_{\ddot{x}}^2$. This means $E\left[\ddot{x}_2^2\right]/\sigma_{\ddot{x}}^2 = E[\ddot{x}_2^2]/E[\ddot{x}_1^2]$. According to Bruce Design Guide (Sengupta, 2005), "From random vibration theory, it is known that maximum response is basically a peak factor times the standard deviation of the random response, and the peak factor is relatively a constant. Also note that variance is square of standard deviation. Therefore, the ordinate ($E\left[\ddot{x}_2^2\right]/\sigma_{\ddot{x}}^2$) of Figure B-1 of Crandall and Mark (1963) is the same as square of the ratio of maximum responses." Thus, Equations (2.59) and (2.65) of Crandall and Mark (1963) lead to the following expression for amplification factor:

$$AF = \sqrt{\frac{E\left[\ddot{x}_2^2\right]}{\sigma_{\ddot{x}}^2}} = \sqrt{\frac{\eta N}{\zeta_2\left(4\zeta_1^2+1\right)D}} \tag{8}$$

Where,

$$\eta = \frac{\omega_2}{\omega_1}$$

$$N = 4\zeta_1\zeta_2(\zeta_2 + \eta\zeta_1)(\eta^2 + 4\zeta_1\zeta_2\eta + 1) + 4\eta(\eta\zeta_1^3 + \zeta_2^3) + \zeta_1 + \eta^3\zeta_2$$

$$D = 4\eta\zeta_1\zeta_2(\eta^2 + 1) + 4\eta^2(\zeta_1^2 + \zeta_2^2) + (\eta^2 - 1)^2$$

Figure 9 shows plots of $E[\ddot{x}_2^2]/\sigma_{\ddot{x}}^2$ with respect to η that match with those in Crandall and Mark (1963).

SCALING OF SPECTRA TO OBTAIN FRS

The fragility guide 3002012994 (EPRI, 2018) recommends the following procedures for simplified and detailed scaling.

Simplified Scaling

Simplified scaling is considered acceptable for rock sites where the spectral shapes of the RLE and the DBE are similar and when only modal frequencies and participation factors are available (from the legacy models). Following steps are reproduced from the guide 3002012994 (EPRI, 2018) in the context of applicable events at Bruce site with few additions, e.g., association of significant modes with their frequencies and the use of acronyms such as DBE and RLE applicable to Bruce site.

1. Evaluate a scale factor as a function of frequency: $Scale\ factor\ (frequency) = RLE/DBE$
2. Use shape of the legacy DBE FRS and the participation factors to deduce significant modes (and frequencies)
3. Scale the legacy DBE FRS and each significant frequency using the above equation. Apply scaling over a ±15% frequency bandwidth.
4. At frequencies below the first significant frequency, the scaled FRS is transitioned to the DBE FRS.
5. Between scaled modes, the new RLE FRS is to generally follow the shape of the DBE FRS.
6. The DBE FRS ZPA is scaled up by the factor for the first significant mode / frequency. From the amplified peak at the highest significant mode frequency out to higher frequencies, the spectra should be transitioned to the scaled ZPA level.

In order to obtain the scaled FRS for the NBK spectrum, the above steps are utilized to scale down the legacy DBE FRS and then scale it up to obtain the RLE FRS. It is to be noted that for scaling down step 6 is inapplicable since the ratio of DBE and NBK spectra =1, at the first significant frequency. Since the DBE spectrum does not contain frequencies above 33Hz unlike NBK, the portion of the spectrum beyond 33Hz is treated separately with two prominent frequencies: 44.54 and 57.172 Hz. This approach reflects the ratio of the peak spectral accelerations of the excitation, i.e. the NBK spectrum, with its ZPA, in the amplified FRS. The accelerations pertaining to both frequencies in the DBE FRS are multiplied by the respective ratios NBK/DBE at these frequencies.

Table 2: Mass normalized participation factors and mode shape ordinates at node 4 in Figure 5

Mode	Freq (Hz)	ϕ	Γ	Effective mass (Γ^2)	Mass participation	$\Gamma\phi$	$\sum \Gamma\phi$
4*	16.971	0.00486	49.2	2420.64	64%	0.24	1
22**	44.54	-0.0207	-36.716	1348.065	36%	0.76	

* (Raj, 1982) ** (Kinectrics, 2011)

Table 3: Simplified scaling details

Freq (Hz)	Selection Basis	Scaling factors*		Net factor	Acceleration (g)
		Down (NBK/DBE)	Up (RLE/DBE)		
7	FRS shape peak	1	1.261	1.261	0.205
16.971	Modal frequency	1	2.739	2.739	0.29
44.54	Modal frequency	0.794	3.803	3.021	0.145
57.172	ZPA	0.66	1.261	0.83	0.04

*Scaling factors due to other reasons such as incoherence, damping etc. are considered as 1.

Looking at the legacy FRS in Figure 6(c) and the mode shape information in Table 2, three prominent frequencies emerge: 7 Hz (peak frequency), 16.97Hz and 44.54 Hz (modal frequencies). Table 3 provides details of predominant frequencies. The scaled factors in Table 3 do not include the effect of damping or any other attributes such as incoherence etc.

Figure 10 shows the scaled spectra for the DBE and NBK spectral excitation. It is seen that the scaled spectrum for NBK excitation is 33% lower than that for the DBE over high frequencies. Mostly the high frequency sensitive components are rigid and by utilizing the NBK spectrum for scaling in vertical direction the extent of condition in a NPP for such components can be mitigated by 33%.

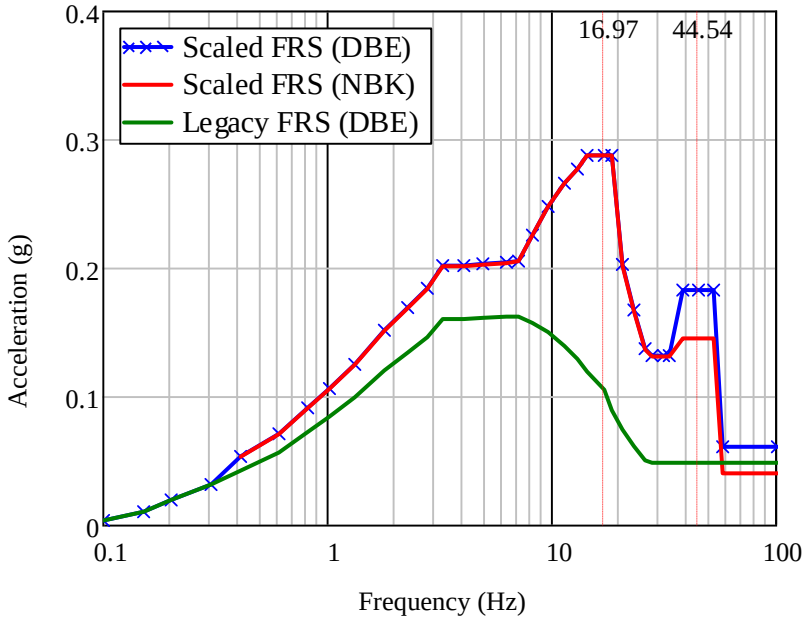

Figure 10: Vertical spectra at Node 4 scaled by spectral acceleration ratios. All other scaling factors =1.

Detailed scaling

The following procedure describes detailed scaling based on Random Vibration Theory (Crandall & Mark, 1963).

1. Use White Noise (WN) Solution of Cascaded SDOF oscillators from Crandall & Mark (1963). See Equation (8).
2. Develop amplification factor, AF, for each modal frequency of the floor oscillator to the structural response at the point of contact from the WN solutions. AF can be calculated by using Equation (8).
3. Evaluate modal floor response as AF $\Gamma\phi$ (0.8) Sag. The 0.8 constant is the ratio of RVT peak factors from literature. Sag is the excitation spectral acceleration.
4. Combine modes and direction components by conventional means to obtain the scaled floor response spectra.

The process to obtain the amplified response spectral (or FRS) acceleration, S_{A_amp} at frequency f_f at node i is summarized in the following equation:

$$S_{A\_amp}(f_f) = \left[\sum_m \left((0.8)AF_j\Gamma_j\phi_{ij}S_{Ag}(f_f)\right)^2\right]^{\frac{1}{2}} \quad (9)$$

Where, f_f is the frequency at which spectral acceleration is desired, AF_j is obtained from Equation (8) for $\eta = (f_f/f_j)$, the ratio of the target frequency with the j^{th} modal frequency, ϕ_{ij} is the j^{th} mode shape ordinate at node i and $S_{Ag}(f_f)$ is the excitation response spectral acceleration (or ground response spectral acceleration in case of a building) at frequency f_f.

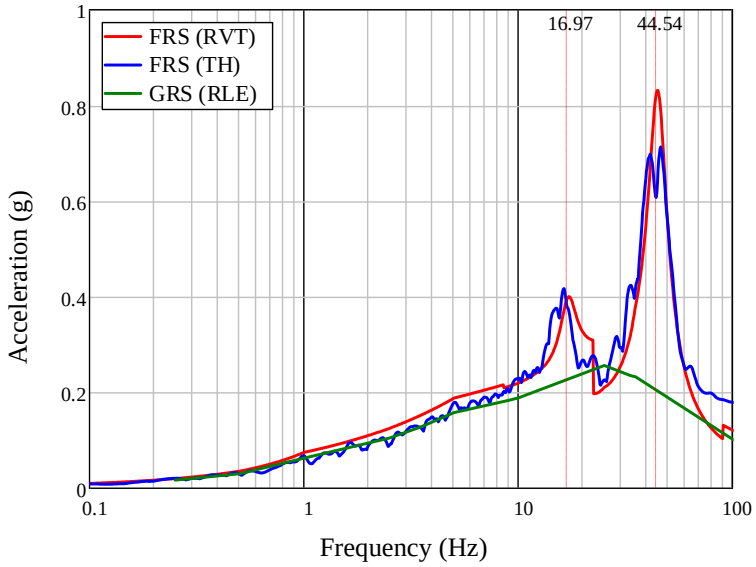

Figure 11: Vertical FRS at Node 4 obtained by random vibration theory and the RLE time history.

Figure 11 shows the raw (unsmoothed, without peak clipping and broadening) FRS at node 4 for the lumped mass in Figure 4 obtained by detailed scaling utilizing random vibration theory and by the dynamic analysis with the RLE time history excitation utilizing the modal frequencies and participation factors in Table 1. As illustrated in Figure 10, the peaks of the spectra match with the modal frequencies. The impact of higher modes amplification is realized at lower nodes in the structure and the peak acceleration is much lesser than the fragilities of high frequency sensitive components reported in the literature (EPRI, 2015).

Peak Amplification Range

It is to be noted that in Equation (9), ideally the amplification factor, AF, should be equal to 1 for modes beyond *rigid* frequency of the excitation spectrum since a rigid oscillator does not amplify or attenuate the base excitation. For the USNRC spectrum there will be no peaks for rigid modes. However, such modes will replicate the response spectrum multiplied by their respective multiplier, $\Gamma\phi$. For the RLE, due to the *rigid* frequency equal to 100 Hz, peak amplification will be visible at higher modes as illustrated in Figure 11. It was observed that the peak correction factor =0.8, in Equation (9), is applicable only to the range $0.5 \leq \eta \leq 2$. This is because per Figure 9, within this range, the amplification is more than 1 and increases rapidly as η approaches 1. However, outside this range its behaviour is quite the opposite, i.e., decreasing slowly. Outside this range including beyond rigid frequency, a constant $AF = 1.5$ produces fairly good results with acceptable conservatism.

Approximate Procedure for Inclusion of Missing Mass

It is to be noted that the sum $\sum \Gamma\phi$ being equal to 1 (the last column of Table 2) is an indication that all prominent modes have been included in the analysis with 100% cumulative mass participation. If the legacy analysis provides information on limited number of modes up to 33 Hz, the missing $\Gamma_{missing}\phi_{missing}$ can be calculated from Equation (4) assuming it to belong to the entire missing mass. If mode shapes are mass normalized, $\Gamma_{missing}$ can be calculated as $\sqrt{\text{Total mass} - \sum \Gamma^2}$. Assuming positive $\Gamma_{missing}$, $\phi_{missing}$ can be calculated. Regarding the frequency for the missing mass excitation, an engineering judgment can be made: 50Hz, for example.

CONCLUSIONS

This study focused on amplification of vertical excitation through the structures in NPPs. The difference between the vertical response spectrum recommended in the USNRC Regulatory Guide 1.60 and the NBK spectrum (Newmark et al. 1973) were highlighted, especially over high frequencies. The equations of both the spectra were formulated. It is concluded that the USNRC vertical spectrum contains inherent conservatism over high frequencies. Utilizing the NBK spectrum in vertical direction reduces the seismic demand over high frequencies. Thus, the extent of condition on seismic demand of high frequency sensitive components can be mitigated by 33% in NPPs, especially where the response spectral shapes of the legacy design basis earthquake and the review level earthquakes are similar. Scaling rules in EPRI report 3002012994 are warranted to include the scaling procedure for the NBK spectrum over high frequencies as suggested in this study.

In this study, the benchmark example given in the EPRI fragility guides 1002988 (EPRI, 2002) and 3002012994 (EPRI, 2018) was revisited at lower nodes. Scaling of response spectrum by random vibration theory was studied and amplification factor equation was formulated. The amplified response spectra at lower nodes in the EPRI guide benchmark example were generated by random vibration theory and response spectrum compatible time history in vertical direction. Both spectra were found to be in agreement. However, at lower nodes, the peak spectral acceleration was found to be much lower than the fragility of high frequency sensitive components reported in the literature. It is concluded that the extent of condition of components affected by high frequency excitation, especially near columns and shear walls, can be mitigated to a large extent by closely examining mode shapes, participation factors and amplification pattern through the height of the structure. Observations made on applicability of amplification factor multiple of 0.8 (recommended by EPRI report 3002012994) within the range $0.5 \leq \eta \leq 2$ and a constant amplification factor of 1.5 outside this range are warranted to be included in EPRI report 3002012994.

The vertical amplification factors provided in the EPRI report 3002004396 (EPRI, 2015) should be investigated for their applicability on higher elevations in a structure because the higher modes lead to high frequency amplification at lower nodes. Whereas at higher elevations, the high frequency content (that is likely to impact high frequency sensitive components such as relays) is filtered out. The current version of EPRI report 3002004396 in its Figure 4-4 recommends a linearly increasing high frequency amplification factor with the increase in height above foundation. This is in contradiction with the observations made in this study. Since the high frequency content is filtered out at higher elevations, the extent of condition of high frequency sensitive components can be further mitigated.

ACKNOWLEDGMENTS

The authors acknowledge Bruce Power for providing resources to write this paper. The opinions, views and conclusions expressed herein are of the authors and are not representative of an official position of Bruce Power.

ACRONYMS

CSA	Canadian Standards Association
DBE	Design Basis Earthquake
ENA	Eastern North America
EPRI	Electric Power Research Institute
NBK	Newmark, Blume and Kapur
NPP	Nuclear Power Plant
MDOF	Multi-Degree-of-Freedom
PGA	Peak Ground Acceleration
PGD	Peak Ground Displacement
RLE	Review Level Earthquake
SMA	Seismic Margin Assessment
SDOF	Single-Degree-of-Freedom
SSE	Safe Shut-down Earthquake
PRA	Probabilistic Risk Assessment
UHRS	Uniform Hazard Response Spectrum
USNRC	United States Nuclear Regulatory Commission
ZPA	Zero period acceleration	

REFERENCES

Atkinson, G. M., & Elgohary, M. (2007). Typical uniform hazard spectra for eastern North American sites at low probability levels. *Canadian Journal of Civil Engineering, 34*, 12-18.

Crandall , S. H., & Mark, W. D. (1963). *Random Vibration in Mechanical Systems.* New York: Academic Press.

CSA. (2010). *CSA N289.3. Design Procedures for Seismic Qualification of CANDU Nuclear Power Plants.* Rexdale, Ontario, Canada: Canadian Standards Association.

Dar, A. (2014). Evaluation of Seismic Design Criteria for Rocking Objects in Nuclear Facilities (Master's thesis). McMaster University.

Dar, A., & Hanna, J. D. (2012). Beyond design basis seismic evaluation of nuclear power plants at Bruce site. *3rd International Structural Specialty Conference.* Edmonton: Canadian Society for Civil Engineering.

Dar, A., Konstantinidis, D., & El-Dakhakhni, W. W. (2014). Station challenges on seismic qualification of structures, systems and components in Canadian nuclear power plants. *Proceedings of the 10th National Conference in Earthquake Engineering.* Anchorage: Earthquake Engineering Research Institute.

EPRI. (1991). *NP-6041-SL-Revision 1. A Methodology for Assessment of Nuclear Power Plant Seismic Margin.* Palo Alto, CA: Electric Power Research Institute.

EPRI. (2002). *Report 1002988, Seismic Fragility Application Guide.* Palo Alto, CA : Electric Power Research Institute.

EPRI. (2015). *Report 3002004396. High Frequency Program: Application Guidance for Functional Confirmation and Fragility Evaluation.* Palo Alto, CA: Electric Power Research Institute.

EPRI. (2018). Report 3002012994: Seismic Fragility and Seismic Margin Guidance for Seismic Probabilistic Risk Assessments. Palo Alto, CA: Electric Power Research Institute.

Kinectrics. (2011). *Bruce Nuclear Generating Station B Seismic PRA Bruce B Reactor Building SSI Structural Model.* K-410003-REPT-0001, Rev 0.

Newmark, N. M., Blume, J. H., & Kapur, K. K. (1973). Seismic Design Spectra for Nuclear Power Plants. *Journal of the Power Division, ASCE*, 287-303.

PTC. (2012). Mathcad 15.0. Parametric Technology Corporation, 140 Kendrick Street, Needham, MA 02494, USA.

Raj, K. (1982). *Bruce GS B Reactor Building Seismic Analysis by Lumped Mass Model.* Ontario Hydro File No. 973 NK29-21001, Report No. 82115 R0.

Sengupta, A. (2005). *Bruce A Nuclear Generating Station Seismic Stuctural Design Guide.*

USNRC. (1973). *Design Response Spectra for Seismic Design of Nuclear Power Plants, Regulatory Guide 1.60, Revision 1.* Washington, D.C.: United States Nuclear Regulatory Commission.

USNRC. (2014). *Design Response Spectra for Seismic Design of Nuclear Power Plants, Regulatory Guide 1.60, Revision 2.* Washington DC: United States Nuclear Regulatory Commission.

APPENDIX

Table A.1: USNRC Reg Guide 1.60 response spectral accelerations (g) scaled to the PGA = 0.05g*

Horizontal										Vertical									
Freq	Damping in percentage									Freq	Damping in percentage								
(Hz)	2	3	4	5	6	7	8	9	10	(Hz)	2	3	4	5	6	7	8	9	10
0.1	0.0046	0.0042	0.004	0.0038	0.0036	0.0035	0.0033	0.0032	0.0031	0.1	0.0031	0.0028	0.0026	0.0025	0.0024	0.0023	0.0022	0.0021	0.0021
0.15	0.0104	0.0095	0.0089	0.0085	0.0081	0.0078	0.0075	0.0073	0.007	0.15	0.0069	0.0064	0.0060	0.0056	0.0054	0.0052	0.0050	0.0048	0.0047
0.2	0.0184	0.0169	0.0159	0.0151	0.0144	0.0138	0.0133	0.0129	0.0125	0.2	0.0123	0.0113	0.0106	0.0100	0.0096	0.0092	0.0089	0.0086	0.0083
0.25	0.0288	0.0265	0.0248	0.0235	0.0225	0.0216	0.0208	0.0201	0.0195	0.25	0.0192	0.0176	0.0165	0.0157	0.0150	0.0144	0.0139	0.0134	0.0130
0.5	0.0526	0.0477	0.0443	0.0416	0.0394	0.0376	0.0359	0.0345	0.0332	0.5	0.0356	0.0324	0.0301	0.0283	0.0269	0.0256	0.0245	0.0236	0.0227
0.75	0.0747	0.0674	0.0622	0.0581	0.0548	0.0519	0.0495	0.0473	0.0453	0.75	0.0512	0.0463	0.0428	0.0400	0.0378	0.0359	0.0343	0.0328	0.0315
1	0.0959	0.0861	0.0791	0.0736	0.0691	0.0654	0.0621	0.0591	0.0565	1	0.0662	0.0596	0.0548	0.0512	0.0482	0.0456	0.0434	0.0415	0.0397
1.25	0.1165	0.1041	0.0953	0.0885	0.0829	0.0781	0.074	0.0703	0.0671	1.25	0.0808	0.0724	0.0665	0.0619	0.0581	0.0549	0.0522	0.0497	0.0475
1.5	0.1364	0.1216	0.111	0.1028	0.0961	0.0904	0.0854	0.081	0.0771	1.5	0.0951	0.0850	0.0779	0.0724	0.0678	0.0640	0.0606	0.0577	0.0550
1.75	0.156	0.1386	0.1263	0.1167	0.1088	0.1022	0.0964	0.0914	0.0868	1.75	0.1091	0.0974	0.0890	0.0825	0.0772	0.0727	0.0688	0.0654	0.0623
2	0.1751	0.1553	0.1412	0.1302	0.1213	0.1137	0.1071	0.1013	0.0961	2	0.1229	0.1095	0.0999	0.0925	0.0864	0.0813	0.0768	0.0729	0.0693
2.25	0.194	0.1717	0.1558	0.1435	0.1334	0.1249	0.1176	0.1111	0.1052	2.25	0.1366	0.1214	0.1107	0.1023	0.0955	0.0897	0.0846	0.0802	0.0762
2.5	0.2126	0.1878	0.1702	0.1565	0.1453	0.1359	0.1277	0.1205	0.1141	2.5	0.1500	0.1332	0.1212	0.1119	0.1043	0.0979	0.0923	0.0874	0.0830
2.75	0.2097	0.1852	0.1679	0.1544	0.1434	0.1341	0.126	0.1189	0.1125	2.75	0.1634	0.1448	0.1316	0.1214	0.1131	0.1060	0.0998	0.0944	0.0896
3	0.2071	0.183	0.1658	0.1525	0.1416	0.1324	0.1245	0.1174	0.1112	3	0.1766	0.1563	0.1419	0.1308	0.1217	0.1139	0.1073	0.1013	0.0961
3.25	0.2048	0.1809	0.1639	0.1508	0.14	0.1309	0.1231	0.1161	0.1099	3.25	0.1897	0.1677	0.1521	0.1400	0.1302	0.1218	0.1146	0.1082	0.1025
3.5	0.2026	0.179	0.1622	0.1492	0.1386	0.1296	0.1218	0.1149	0.1088	3.5	0.2027	0.1790	0.1622	0.1492	0.1386	0.1296	0.1218	0.1149	0.1087
3.75	0.2007	0.1772	0.1606	0.1477	0.1372	0.1283	0.1206	0.1138	0.1077	3.75	0.2007	0.1772	0.1606	0.1477	0.1372	0.1283	0.1206	0.1138	0.1077
4	0.1988	0.1756	0.1592	0.1464	0.1359	0.1271	0.1195	0.1127	0.1067	4	0.1988	0.1756	0.1592	0.1464	0.1359	0.1271	0.1195	0.1127	0.1067
6	0.1877	0.1658	0.1502	0.1382	0.1283	0.12	0.1128	0.1064	0.1007	6	0.1877	0.1658	0.1502	0.1382	0.1283	0.1200	0.1128	0.1064	0.1007
8	0.1801	0.1591	0.1442	0.1326	0.1232	0.1152	0.1082	0.1021	0.0967	8	0.1801	0.1591	0.1442	0.1326	0.1232	0.1152	0.1082	0.1021	0.0967
9	0.1771	0.1565	0.1418	0.1304	0.1211	0.1133	0.1064	0.1004	0.0951	9	0.1771	0.1565	0.1418	0.1304	0.1211	0.1133	0.1064	0.1004	0.0951
11	0.1457	0.1312	0.1207	0.1125	0.1056	0.0998	0.0947	0.0902	0.0861	11	0.1457	0.1312	0.1207	0.1125	0.1056	0.0998	0.0947	0.0902	0.0861
13	0.1238	0.1133	0.1056	0.0994	0.0943	0.0899	0.0859	0.0824	0.0793	13	0.1238	0.1133	0.1056	0.0994	0.0943	0.0899	0.0859	0.0824	0.0793
15	0.1077	0.0999	0.0941	0.0895	0.0855	0.0821	0.0791	0.0763	0.0738	15	0.1077	0.0999	0.0941	0.0895	0.0855	0.0821	0.0791	0.0763	0.0738
17	0.0954	0.0895	0.0851	0.0816	0.0785	0.0759	0.0735	0.0714	0.0694	17	0.0954	0.0895	0.0851	0.0816	0.0785	0.0759	0.0735	0.0714	0.0694
19	0.0856	0.0812	0.0779	0.0751	0.0728	0.0708	0.0689	0.0672	0.0657	19	0.0856	0.0812	0.0779	0.0751	0.0728	0.0708	0.0689	0.0672	0.0657
21	0.0776	0.0744	0.0719	0.0698	0.068	0.0664	0.065	0.0637	0.0625	21	0.0776	0.0744	0.0719	0.0698	0.0680	0.0664	0.0650	0.0637	0.0625
23	0.0711	0.0686	0.0668	0.0653	0.0639	0.0628	0.0617	0.0607	0.0598	23	0.0711	0.0686	0.0668	0.0653	0.0639	0.0628	0.0617	0.0607	0.0598
25	0.0655	0.0638	0.0625	0.0614	0.0604	0.0595	0.0588	0.058	0.0574	25	0.0655	0.0638	0.0625	0.0614	0.0604	0.0595	0.0588	0.0580	0.0574
27	0.0608	0.0596	0.0587	0.058	0.0573	0.0567	0.0562	0.0557	0.0552	27	0.0608	0.0596	0.0587	0.0580	0.0573	0.0567	0.0562	0.0557	0.0552
29	0.0567	0.056	0.0555	0.055	0.0546	0.0542	0.0539	0.0536	0.0533	29	0.0567	0.0560	0.0555	0.0550	0.0546	0.0542	0.0539	0.0536	0.0533
31	0.0531	0.0528	0.0526	0.0524	0.0522	0.052	0.0519	0.0517	0.0516	31	0.0531	0.0528	0.0526	0.0524	0.0522	0.0520	0.0519	0.0517	0.0516
33	0.05	0.05	0.05	0.05	0.05	0.05	0.05	0.05	0.05	33	0.0500	0.0500	0.0500	0.0500	0.0500	0.0500	0.0500	0.0500	0.0500
35	0.05	0.05	0.05	0.05	0.05	0.05	0.05	0.05	0.05	35	0.0500	0.0500	0.0500	0.0500	0.0500	0.0500	0.0500	0.0500	0.0500
100	0.05	0.05	0.05	0.05	0.05	0.05	0.05	0.05	0.05	100	0.0500	0.0500	0.0500	0.0500	0.0500	0.0500	0.0500	0.0500	0.0500

*The user to verify these numbers by plotting them together with the USNRC spectra on log-log scale.